



HAL
open science

Laser-induced breakdown spectroscopy enhanced by a micro torch

Lei Liu, Xi Huang, Shuo Li, Yao Lu, Kevin Chen, Lan Jiang, Jean-François Silvain, Yong Feng Lu

► **To cite this version:**

Lei Liu, Xi Huang, Shuo Li, Yao Lu, Kevin Chen, et al.. Laser-induced breakdown spectroscopy enhanced by a micro torch. *Optics Express*, 2015, 23 (11), pp.15047-15056. 10.1364/OE.23.015047 . hal-01160308

HAL Id: hal-01160308

<https://hal.science/hal-01160308>

Submitted on 26 Jan 2021

HAL is a multi-disciplinary open access archive for the deposit and dissemination of scientific research documents, whether they are published or not. The documents may come from teaching and research institutions in France or abroad, or from public or private research centers.

L'archive ouverte pluridisciplinaire **HAL**, est destinée au dépôt et à la diffusion de documents scientifiques de niveau recherche, publiés ou non, émanant des établissements d'enseignement et de recherche français ou étrangers, des laboratoires publics ou privés.



Distributed under a Creative Commons Attribution - NonCommercial - NoDerivatives 4.0 International License

Laser-induced breakdown spectroscopy enhanced by a micro torch

L. Liu,¹ X. Huang,¹ S. Li,² Yao Lu,¹ K. Chen,² L. Jiang,³ J.F. Silvain,^{1,4} and Y.F. Lu^{1,*}

¹ Department of Electrical and Computer Engineering, University of Nebraska-Lincoln, Lincoln, NE 68588-0511 USA

² Department of Electrical and Computer Engineering, University of Pittsburgh, Pittsburgh, PA 15260 USA

³ School of Mechanical Engineering, Beijing Institute of Technology, 100081, China

⁴ Institut de Chimie de la Matière Condensée de Bordeaux – ICMCB-CNRS 87, Avenue du Docteur Albert Schweitzer F-33608 Pessac Cedex, France
*ylu2@unl.edu

Abstract: A commercial butane micron torch was used to enhance plasma optical emissions in laser-induced breakdown spectroscopy (LIBS). Fast imaging and spectroscopic analyses were used to observe plasma evolution in the atmospheric pressure for LIBS without and with using a micro torch. Optical emission intensities and signal-to-noise ratios (SNRs) as functions of delay time were studied. Enhanced optical emission and SNRs were obtained by using a micro torch. The effects of laser pulse energy on the emission intensities and SNRs were studied. The same spectral intensity could be obtained using micro torch with much lower laser pulse energy. The investigation of SNR evolution with delay time at different laser pulse energies showed that the SNR enhancement factor is higher for plasmas generated by lower laser pulse energies than those generated by higher laser energies. The calibration curves of emission line intensities with elemental concentrations showed that detection sensitivities of Mn I 404.136 nm and V I 437.923 nm were improved by around 3 times. The limits of detection for both Mn I 404.136 nm and V I 437.923 nm are reduced from 425 and 42 ppm to 139 and 20 ppm, respectively, after using the micro torch. The LIBS system with micro torch was demonstrated to be cost-effective, compact, and capable of sensitivity improvement, especially for LIBS system operating with low laser pulse energy.

©2015 Optical Society of America

OCIS codes: (300.6365) Spectroscopy, laser induced breakdown; (350.5400) Plasmas.

References and links

1. R. Noll, *Laser-Induced Breakdown Spectroscopy* (Springer, 2012).
2. A. W. Miziolek, V. Palleschi, and I. Schechter, *Laser-Induced Breakdown Spectroscopy (LIBS)* (Cambridge University Press Cambridge, 2006).
3. J. P. Singh and S. N. Thakur, *Laser-Induced Breakdown Spectroscopy* (Elsevier, 2007).
4. V. I. Babushok, F. C. DeLucia, Jr., J. L. Gottfried, C. A. Munson, and A. W. Miziolek, "Double pulse laser ablation and plasma: Laser induced breakdown spectroscopy signal enhancement," *Spectrochim. Acta, Part B* **61**(9), 999–1014 (2006).
5. R. W. Coons, S. S. Harilal, S. M. Hassan, and A. Hassanein, "The importance of longer wavelength reheating in dual-pulse laser-induced breakdown spectroscopy," *Appl. Phys. B* **107**(3), 873–880 (2012).
6. J. Scaffidi, J. Pender, W. Pearman, S. R. Goode, B. W. Colston, Jr., J. C. Carter, and S. M. Angel, "Dual-pulse laser-induced breakdown spectroscopy with combinations of femtosecond and nanosecond laser pulses," *Appl. Opt.* **42**(30), 6099–6106 (2003).
7. W. Zhou, K. Li, X. Li, H. Qian, J. Shao, X. Fang, P. Xie, and W. Liu, "Development of a nanosecond discharge-enhanced laser plasma spectroscopy," *Opt. Lett.* **36**(15), 2961–2963 (2011).
8. W. Zhou, K. Li, Q. Shen, Q. Chen, and J. Long, "Optical emission enhancement using laser ablation combined with fast pulse discharge," *Opt. Express* **18**(3), 2573–2578 (2010).
9. Y. A. Liu, M. Baudalet, and M. Richardson, "Elemental analysis by microwave-assisted laser-induced breakdown spectroscopy: evaluation on ceramics," *J. Anal. At. Spectrom.* **25**(8), 1316–1323 (2010).

10. M. Tampo, M. Miyabe, K. Akaoka, M. Oba, H. Ohba, Y. Maruyama, and I. Wakaida, "Enhancement of intensity in microwave-assisted laser-induced breakdown spectroscopy for remote analysis of nuclear fuel recycling," *J. Anal. At. Spectrom.* **29**(5), 886–892 (2014).
 11. R. Sanginés, H. Sobral, and E. Alvarez-Zauco, "Emission enhancement in laser-produced plasmas on preheated targets," *Appl. Phys. B* **108**(4), 867–873 (2012).
 12. L. B. Guo, W. Hu, B. Y. Zhang, X. N. He, C. M. Li, Y. S. Zhou, Z. X. Cai, X. Y. Zeng, and Y. F. Lu, "Enhancement of optical emission from laser-induced plasmas by combined spatial and magnetic confinement," *Opt. Express* **19**(15), 14067–14075 (2011).
 13. L. B. Guo, B. Y. Zhang, X. N. He, C. M. Li, Y. S. Zhou, T. Wu, J. B. Park, X. Y. Zeng, and Y. F. Lu, "Optimally enhanced optical emission in laser-induced breakdown spectroscopy by combining spatial confinement and dual-pulse irradiation," *Opt. Express* **20**(2), 1436–1443 (2012).
 14. X. K. Shen, Y. F. Lu, T. Gebre, H. Ling, and Y. X. Han, "Optical emission in magnetically confined laser-induced breakdown spectroscopy," *J. Appl. Phys.* **100**(5), 053303 (2006).
 15. X. K. Shen, J. Sun, H. Ling, and Y. F. Lu, "Spatial confinement effects in laser-induced breakdown spectroscopy," *Appl. Phys. Lett.* **91**(8), 081501 (2007).
 16. L. Liu, S. Li, X. N. He, X. Huang, C. F. Zhang, L. S. Fan, M. X. Wang, Y. S. Zhou, K. Chen, L. Jiang, J. F. Silvain, and Y. F. Lu, "Flame-enhanced laser-induced breakdown spectroscopy," *Opt. Express* **22**(7), 7686–7693 (2014).
 17. J. D. Ingle and S. R. Crouch, *Spectrochemical Analysis* (Prentice-Hall, 1988).
 18. H. R. Griem, *Spectral Line Broadening by Plasmas* (Academic Press, 1974).
 19. Q. Zeng, L. Guo, X. Li, C. He, M. Shen, K. Li, J. Duan, X. Zeng, and Y. Lu, "Laser-induced breakdown spectroscopy using laser pulses delivered by optical fibers for analyzing Mn and Ti elements in pig iron," *J. Anal. At. Spectrom.* **30**(2), 403–409 (2015).
 20. D. A. Cremers, F. Y. Yueh, J. P. Singh, and H. Zhang, *Laser-Induced Breakdown Spectroscopy, Elemental Analysis* (Wiley Online Library, 2006).
-

1. Introduction

Laser-induced breakdown spectroscopy (LIBS) is a spectroscopic technique for elemental analyses. In LIBS, a pulsed laser is focused on a target surface to ablate the target and induce plasmas. Plasma emissions containing elemental information of the target are collected for spectroscopic analyses [1]. LIBS has been proven to be a versatile tool during the past decades in the fields of industry, biological chemistry, life science, space exploration, archaeology, etc., due to its advantages of no sample preparation and nearly non-destructive measurement, capabilities of multi-element analysis, in situ analysis, and remote detection [2, 3]. However, the limit of detection (LOD) of LIBS is about a few to thousands of ppm, which varies with experimental parameters for different types of elements and species [2]. Works need to be done to improve the sensitivity for detection of trace-level elements, which mainly relies on optical emissions of laser-induced plasmas. Many works have been done by modifying the plasmas to enhance optical emission and improve sensitivity. It has been reported that dual-pulse LIBS has the capability to enhance optical emission using a second laser to re-ablate and reheat the laser-induced plasmas [4–6]. Some other methods, such as LIBS combined with discharge pulse [7, 8], microwave-assisted LIBS [9, 10], optical emission enhancement from preheated targets [11], spatial or magnetic confinement [12–15], have been reported to enhance optical emission. However, most of these methods suffer from system complexity or operation inconvenience. Our previous work [16] also reported optical emission enhancement in LIBS with generated plasmas expanding in a high-temperature flame environment.

In this study, unlike the high-temperature flame generated by mixed fuels used in our previous work, a commercial butane micro torch which generates a smaller size flame was used. The micro torch is cost-effective, compact, and portable. Besides the observed optical emission enhancement, the signal-to-noise ratio (SNR) enhancement was also studied. Also the effects of laser pulse energy on the optical emission and SNRs were studied. The calibration curves of the relationship between optical emission intensities and elemental concentrations for both Mn I 404.136 nm and V I 437.923 nm in steel targets were established for estimating LODs. The LIBS with micro torch is cost-effective, portable and capable of improving sensitivity for detecting trace-level elements, especially for low laser pulse energies.

2. Experiment setup

The schematic diagram of the LIBS system with micro torch is shown in Fig. 1. A Q-switched Nd:YAG laser operating at 532 nm (Continuum, Powerlite Precision II 8010, pulse duration of 6 ns) with a repetition rate of 10 Hz was used to induce plasmas on target surfaces. The laser beam was normally focused below the target surface by lens 1 (L1 with 20 cm focal length) to avoid breakdown of the micro flame. The defocused laser spot size on the target surface is 0.8 mm in diameter. A commercial butane micro torch (ST2200T, Bernzomatic) was used to generate a micro flame. The total size of the micro flame is around 0.6×4 cm and the inner flame size is around 0.3×1.5 cm. This geometry flame size is divided by the flame color with the blue opaque part as inner flame and the dark transparent part as outer flame. The outer flame temperature is about 1700K. The assembled size of the micro torch is around 3.0 inch \times 5.8 inch, which provides the advantage of portability and convenience of operation. Laser-induced plasmas expanded in the outer envelope of the butane micro flame, as shown in Fig. 1. The plasma position is in the outer flame with about 0.5 cm the inner flame. Plasma emissions were collected by lens 2 (L2 with 6-cm focal length) and lens 3 (L3 with 10-cm focal length) and coupled into a spectrometer (Andor Tech., Shamrock 505i). A 1200 lines/mm grating blazed at 300 nm was used for spectral acquisition with a resolution of 0.06 nm. The spectrometer slit width was set as 2500 and 25 μ m for acquisition of plasma images and spectra, respectively. A 1024 \times 1024 pixel intensified charge coupled device (ICCD) detector (Andor Tech., iStar, DT-334T) was attached to the exit focal plane of the spectrometer. The ICCD detector was operated in the gated mode so that the gate delay and gate width could be adjusted for different measurements. The spectrometer and laser were synchronized by a digital delay generator (Stanford Research System DG 535, 5 ps delay resolution).

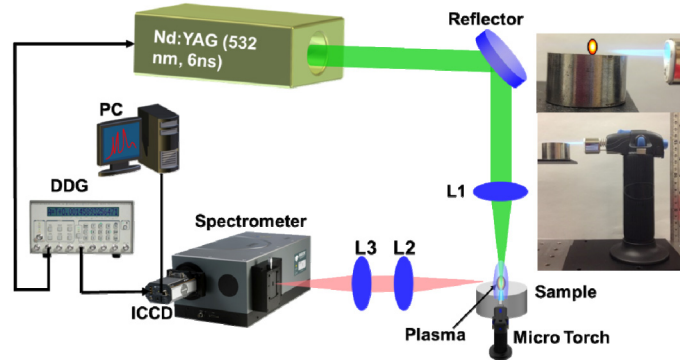


Fig. 1. Schematic diagram of LIBS system using a micro torch. The inserted magnified image (upper) shows the plasma position in the torch flame, in the outer flame with about 0.5 cm to the inner flame end. The magnified image (bottom) shows the micro torch position to sample.

Table 1. Elemental concentrations (wt.%) of Mn and V in steels

Elements	SRMs (wt %)			
	No. 1269	No. 1762	No. 1262b	No. C1285
V	0.004	0.200	0.041	0.150
Mn	1.350	2.000	1.050	0.332

Four steel standard reference materials (SRMs 1269, 1262b, 1762, C1285) from NIST were used as the targets in this study. The matrix element in the steel samples is iron with a content of over 90%. The low-concentration elements of manganese (Mn) and vanadium (V) were chosen for quantitative analyses. The concentrations of both Mn and V in the steel targets are shown in Table 1.

3. 3. Results and discussion

3.1 Fast imaging of plasmas

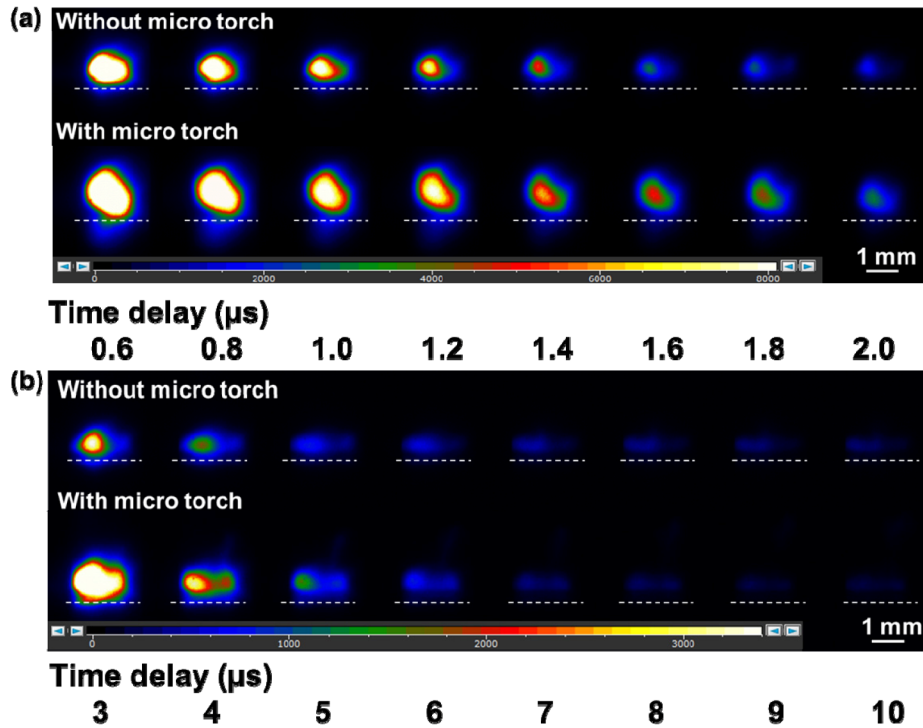


Fig. 2. Instant images of plasma evolution in LIBS without (top row) and with (bottom row) the micro torch (a) from 0.6 to 2.0 μs acquired with a gate width of 0.1 μs and a gate step of 0.2 μs ; and (b) from 3 to 10 μs acquired with a gate width of 0.5 μs and a gate step of 1 μs .

A steel (NIST 1262b) sample and a laser pulse energy of 20 mJ were used to study the image and spectroscopic evolution of the plasmas in LIBS without and with the micro torch. To better observe the effects of micro flame on the plasma evolution, a small gate width of 0.1 μs and a small gate step of 0.2 μs were used for acquisition of images in the early plasma lifetime of 0.6 ~2.0 μs . A larger gate width of 0.5 μs and a larger gate step of 1.0 μs were used for plasma image acquisition in the time range of 3 ~10 μs . Figures 2(a) and 2(b) shows the images of plasma evolution in the time ranges of 0.6 to 2.0 μs and 3 to 10 μs , respectively, without (top row) and with (bottom row) micro torch. The dash lines indicate the location of the target surface. The images are shown in different intensity scales in (a) and (b). For plasma evolution in the early lifetime, as seen in Fig. 2(a), the brightness of the plasma before 0.8 μs is close for LIBS without and with micro torch since the plasma emission is very strong at that time. A relatively larger plasma emission area was also noticed from LIBS with micro torch at that time. Plasma emission enhancement was observed after 1.0 μs . For plasma evolution in the time range of 3 ~10 μs , as shown in Fig. 2(b), obvious enhancement of plasma emission intensity was obtained from 2 to 6 μs and no enhancement or even weaker plasma emission were shown after 6 μs .

3.2 Emission intensity and signal-to-noise ratio (SNR)

The analyses of optical emission intensity and signal-to-noise ratio (SNR) evolution were also studied. Figure 3(a) shows the Mn I 404.136 nm peak intensity as a function of delay time without (black curve with squared dots) and with (red curve with circle dots) the micro torch in the time range of 1 ~10 μs (acquired with a gate width of 0.5 μs). The inserted figure

shows the relationship of optical emission intensity and delay time in the early plasma lifetime of 0.4 ~2.2 μs acquired with a gate width of 0.1 μs . The slit width of 25 μm was set for the measurements. The spectra were accumulated by 10 pulses to reduce the standard deviation of the background. In Fig. 3(a), obvious enhancement of emission line intensity was observed in the initial 6 μs .

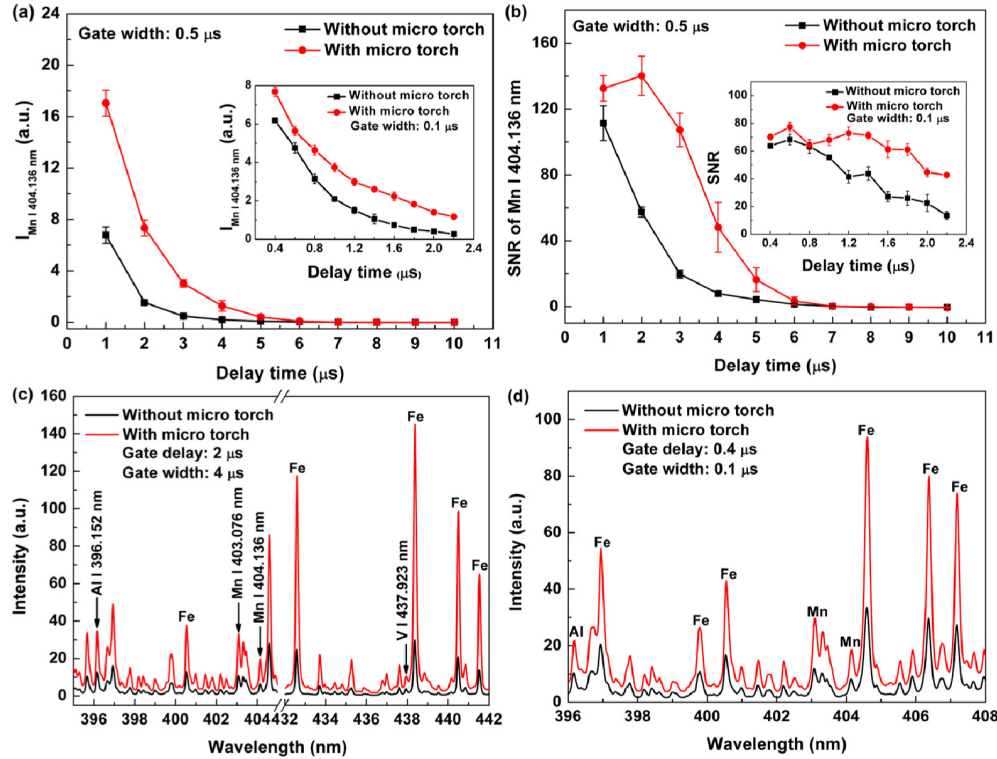


Fig. 3. The relationships between Mn I 404.136 nm (a) optical emission intensities and (b) signal-to-noise ratios (SNR) and the delay times in the time range of 1 ~10 μs without (black curve with squared dots) and with (red curve with circle dots) the micro torch. The inserted figures show the optical emission intensity and SNR evolution in the early plasma lifetime of 0.4 ~2.2 μs . LIBS spectra from SRM 1262b without (black curve) and with (red curve) the micro torch at the delay time of (c) 2 μs and (d) 0.4 μs .

Besides the optical emission intensity evolution, the signal-to-noise ratio (SNR) as a function of the delay time was also investigated since it was related to the detection sensitivity. The SNR was defined as the ratio of the emission intensity to the standard deviation of background [17]. The spectral range from 436.20 to 436.45 nm was chosen as the blank background in this work. The relationship between SNR of Mn I 404.136 nm and the delay time is shown in Fig. 3(b). The inserted figure shows the SNR evolution in the early plasma lifetime of 0.4 ~2.2 μs acquired with a small gate width of 0.1 μs . Figure 3(b) shows that the SNR is greatly enhanced with in the delay time range of 1 ~6 μs with a maximum enhancement of around 5 times. The SNR enhancement was not obvious before 0.8 μs although the emission intensity enhancement was also obtained. The a little bit enhanced continuum background and less enhanced line emission intensity both contributed to the almost no SNR enhancement before 0.8 μs . The spectra at the early plasma lifetime of 0.4 μs were shown in Fig. 4(d).

LIBS spectra without and with the micro torch were measured to show the emission intensity enhancement for low-concentration elements in the steel targets. Figure 3(c) shows

the LIBS spectra from SRM 1262b in a spectral range of 395-442 nm without (black solid line) and with (red solid line) the micro torch. A gate delay of 2 μ s and a gate width of 4 μ s were used in the measurement with the accumulation of 10 pulses. The emission intensities of several low-concentration elements were investigated. As seen in Fig. 3(c), the emission intensity for the atomic line of Al I 396.15 nm (with Al concentration of 0.081%), Mn I 404.136 nm (with Mn concentration of 1.05%), and V I 437.923 nm (with V concentration of 0.041%) are all enhanced by the micro torch. The enhanced emission line intensities and SNRs of low-concentration elements indicate the capability for improving the detection sensitivity

3.3 Plasma temperature and electron density

Electron temperature of plasma and electron density has been estimated to understand the enhancement mechanism. According to the local temperature equilibrium (LTE) and optical thin assumption, measurement of the intensities of a series of lines from different excitation states of the same species allows evaluation of the plasma temperature according to the Boltzmann plot equation [2]

$$\ln \frac{I_{ij}}{g_i A_{ij}} = \ln \left(\frac{n^s}{U^s(T)} \right) - \frac{E_i}{kT} \quad (1)$$

where I_{ij} is the integrated line intensity, A_{ij} , g_i and E_i are the transition probability, statistical weight and excited energy for upper level, respectively, k is the Boltzmann constant, T is the plasma temperature, n^s is the total number density of the species s in the plasma, $U^s(T)$ is the internal partition function of the species at temperature T . The plot of the left-hand side of equation vs. E_i has a slope of $-1/kT$. The plasma temperature can be obtained via linear regression without knowing n^s or $U^s(T)$. Seven lines from atomic iron lines of 390.295, 392.792, 393.030, 396.926, 400.524, 406.359 and 407.174 nm were used for plasma temperature estimation. The parameters of used atomic lines for temperature calculation are shown in Table 2.

For typical LIBS conditions, the contribution from ion broadening is negligible and the equation [2]

$$\Delta\lambda_{\text{stark}} = 2\omega \left(\frac{n_e}{10^{16}} \right) \quad (2)$$

can be used to derive the electron density by assuming that other sources of broadening (natural, Doppler, etc.) are negligible (i.e. $\Delta\lambda_{\text{line}} \cong \Delta\lambda_{\text{stark}}$). The value of ω , the electron impact half-width, can be found in the extensive tables given by Griem [18].

Table 2. Parameters of atomic lines used for plasma temperature calculation

Wavelength (nm)	Excited upper level energy E_i (cm^{-1})	Transition probability A_{ij} (s^{-1})	Statistical weight for upper level g_i
390.295	38175.355	2.14e + 07	7
392.792	26339.696	2.60e + 06	5
393.030	26140.179	1.99e + 06	7
396.926	37162.746	2.26e + 07	7
400.524	37521.161	2.04e + 07	5
406.369	37162.746	6.65e + 07	7
407.174	37521.161	7.64e + 07	5

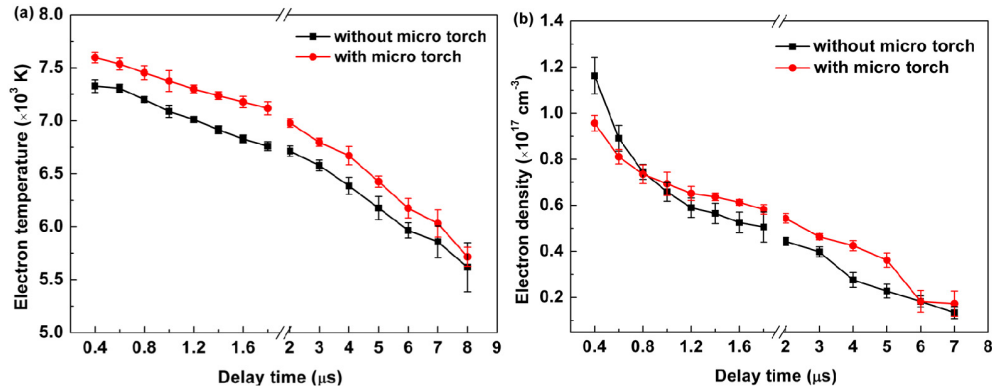


Fig. 4. The relationships between (a) electron temperature and (b) electron density and delay times without (black squared dots) and with (red circle dots) micro torch.

The obtained relationships between electron temperature and electron density and delay times without (black squared dots) and with (red circle dots) micro torch are shown in Figs. 4(a) and 4(b), respectively. The spectra used for calculation were acquired with a gate width of 0.1 μ s before 2 μ s and a gate width of 0.5 μ s after that. Figure 4(a) shows that the plasma temperature is higher in the initial several microseconds with micro torch. Figure 4(b) shows that the electron density is lower in the initial hundreds of nanoseconds (before 0.8 μ s) and higher after that with micro torch. This higher plasma temperature and electron density in the initial several microseconds explains the enhancement effect. The higher plasma temperature but lower electron density in the initial hundreds of nanoseconds explains the less enhanced line emission intensity before 0.8 μ s.

3.4 The effects of laser pulse energy

The effects of laser pulse energy on the optical emission intensities and SNRs were investigated. Figure 5(a) shows the relationship between Mn I 404.136 nm emission intensities and delay times measured with a gate width of 1 μ s from LIBS with micro torch at the laser energies of 10, 20, 30 and 40 mJ and LIBS without micro torch at the laser energy of 40 mJ. The slit width for the measurement was 25 μ m. The accumulation for spectra acquisition is 10 pulses. As seen in Fig. 5(a), the emission intensity with the micro torch at a laser pulse energy of 20 mJ is close to (even a little bit higher) that without a micro torch at the laser pulse energy of 40 mJ due to optical emission enhancement. LIBS spectra measured with the micro torch (red solid line) at the laser pulse energy of 20 mJ and without a micro torch (black solid line) at the laser pulse energy of 40 mJ are shown in Fig. 5(c), which show comparable spectral intensities. This indicates the capability of obtaining high intensity spectra at low laser pulse energy using the micro torch, which is beneficial to LIBS under the conditions of using lasers with low pulse energy, such as those used in portable LIBS systems. Images of plasmas were also measured with the slit width of 2500 μ m, as shown in Fig. 5(d), at the laser energies of 20 (left column) and 40 mJ (right column) from LIBS without (top row) and with (bottom row) the micro torch both with a gate delay of 2 μ s and a gate width of 0.2 μ s. Similarly to the results from spectroscopic analyses, comparable plasma emission intensity was obtained with the micro torch at the laser pulse energy of 20 mJ and without a micro torch at the laser pulse energy of 40 mJ due to enhanced plasma emission intensity with the presence of the micro flame. From the images, we can also observe that the plasma expands faster upwardly and is brighter in torch flame.

The relationship between SNRs enhancement and delay times at different laser energies was investigated. The SNR enhancement factor was defined as the ratio of the averaged SNR value obtained with the micro torch to that without a micro torch. Figure 5(b) shows the

relationship between SNR enhancement factors and Mn I 404.136 nm with delay times at the laser energies of 10, 20, 30 and 40 mJ. Due to the weak line intensity and fast decay at the laser pulse energy of 10 mJ, the SNR enhancement was shown only before 4 μ s. The measurement was carried out with a gate width of 1 μ s and the accumulation of 10 pulses. At the early plasma lifetime of 1 μ s, SNR enhancement was obvious (enhancement factor larger than 1) for lower laser energies of 10 and 20 mJ and not obvious for higher laser energies of 30 and 40 mJ. This could be caused by the fact that the continuum emission at the early delay time of 1 μ s was stronger for plasmas induced by higher laser energy and the continuum emission was also enhanced along with the emission line intensity. Hence the SNR enhancement was not obvious at the early plasma lifetime of 1 μ s when higher laser energy was used. Besides, a trend of higher maximum SNR enhancement factor at lower laser energies was noticed, which indicates that the SNR enhancement effects work better with lower laser pulse energy. A maximum SNR enhancement factor of around 5 times was achieved at the laser energy of 20 mJ. Since both the SNR value and enhancement factor are higher in the early plasma lifetime of several microseconds, the LIBS using micro torch has greater potential of sensitivity improvement for lasers with lower pulse energies.

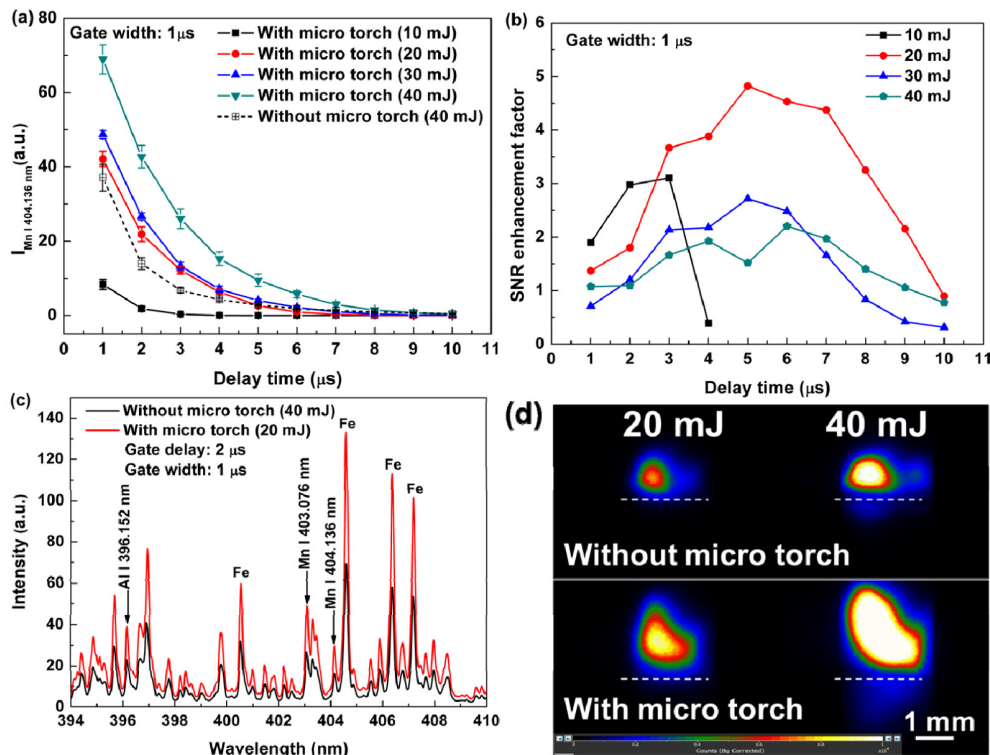


Fig. 5. (a) The relationships between Mn I 404.136 nm emission intensities and the delay times at different laser pulse energies; (b) the relationships between Mn I 404.136 nm SNR enhancement factors and the delay times at different laser pulse energies; (c) LIBS spectra without micro torch (black solid line) at a laser energy of 40 mJ and with the micro torch (red solid line) at a laser energy of 20 mJ; (d) Images of plasma without (top row) and with (bottom row) micro torch at a laser energy of 20 (left column) and 40 mJ (right column), respectively.

3.4 Improved limits of detection of Mn and V in steel targets

Quantitative analyses for low-concentration elements of Mn (0.332 - 2.000%) and V (0.004 - 0.200%) in the previously mentioned four steel samples were investigated. By considering both the SNR value and the SNR enhancement factor, the laser energy of 20 mJ was used for

quantitative analyses. A gate delay of 2 μs and a gate width of 4 μs were used for spectrum acquisition. The LODs for low-concentration Mn and V in steel targets were estimated. The atomic lines of Mn I 403.136 nm and V I 437.923 nm were chosen for quantitative calculation. Figures 6(a) and 6(b) shows the calibration curves between the emission line intensities and elemental concentrations in steel targets for Mn I 403.416 nm and V I 437.923 nm, respectively, for LIBS without (black squares) and with (red circles) the micro torch. As observed in Fig. 6, improved detection sensitivity (larger slope of the calibration curves) for Mn and V was shown in LIBS with the micro torch.

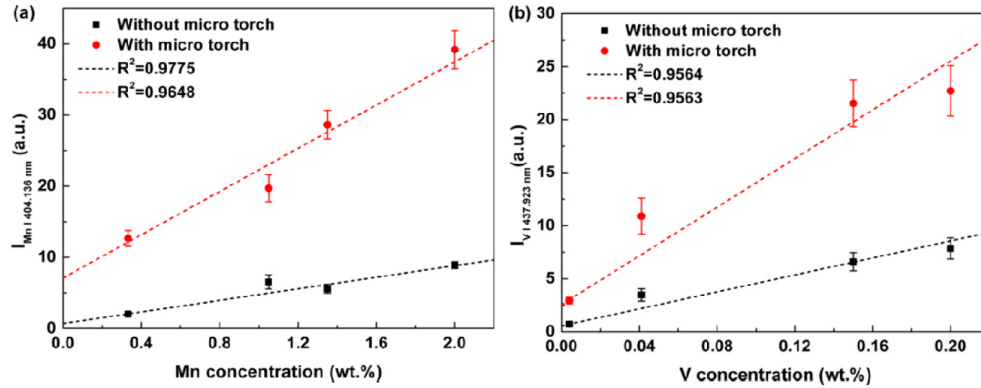


Fig. 6. Calibration curves of the relationship between emission line intensities and elemental concentrations in steel samples for (a) Mn I 404.136 nm; and (b) V I 437.923 nm without (black line with squared dots) and with (red line with circle dots) the micro torch.

To estimate the LODs of Mn and V in the steel samples, the 3σ -International Union of Pure and Applied Chemistry (IUPAC) criteria was used according to the formula [3, 19, 20]:

$$\text{LOD} = 3\sigma_B / S \quad (3)$$

where σ_B is the standard deviation of the background; S is the slope of the calibration curve. The LODs of V and Mn in steel samples were calculated and listed in Table 3. Table 3 shows the R-square factors (R^2), the slope (S) of the calibration curves and the LODs of Mn and V in steel targets. As shown in Table 3, the slopes of calibration curves were enhanced by around 3 times in LIBS with the micro torch, which demonstrated the improvement of the detection sensitivity. The estimated LODs of Mn I 404.136 nm and V I 437.923 nm in steel samples were reduced from 425 and 42 ppm in LIBS without a micro torch to 139 and 20 ppm in LIBS with the micro torch, respectively. The LIBS system with the micro torch demonstrated the capability of improving detection sensitivity and reducing LODs for low concentration elements in steel targets.

Table 3. The R-square (R^2) factor, slope (S) of calibration curve and LODs of Mn and V in LIBS without and with micro torch

Elements	R^2		S (counts/ppm)		LOD (ppm)	
	Without micro torch	With micro torch	Without micro torch	With micro torch	Without micro torch	With micro torch
V	0.9564	0.9563	4.0	11.5	42	20
Mn	0.9775	0.9648	0.4	1.5	425	139

4. Conclusions

In this work, LIBS using a micro torch was used to enhance optical emission and improve detection sensitivity. Fast imaging and spectroscopic analyses were used to investigate the

plasma evolution. Images of plasma evolution show that plasma emission intensities are enhanced before 6 μs with the presence of the micro flame and no enhancement after that. Consistent results were also obtained from spectroscopic analyses of optical emission intensity of the Mn I 404.136 nm. LIBS spectra show that emission intensities of low-concentration elements in steel targets, such as Al, Mn, and V, are all greatly enhanced. The relationship between SNRs and the delay times of Mn I 404.136 nm shows that SNRs are enhanced before 6 μs , with a maximum enhancement of around 5 times at the laser pulse energy of 20 mJ. The effects of laser pulse energy on the optical emission and SNRs were also studied. Due to the optical enhancement effects, comparable spectra intensity was obtained in LIBS with the micro torch at a lower laser pulse energy of 20 mJ to that without a micro torch at a laser pulse energy of 40 mJ. Laser energy effect on SNR shows the trend of higher maximum SNR enhancement factors for lower laser energies. A maximum SNR enhancement factor of around 5 times at the laser pulse energy of 20 mJ was achieved. Quantitative analyses of low-concentration Mn I 404.136 nm and V I 437.923 nm in steel targets show that improved detection sensitivity of around 3 times was achieved using the micro torch. The estimated LODs of both Mn I 404.136 nm and V I 437.923 nm in steel are reduced from 425 and 42 ppm to 139 and 20 ppm, respectively, by using the micro torch. LIBS using a micro torch has the advantages of cost-effectiveness, compactness, portability and capability of improving detection sensitivity, especially for LIBS operating with low laser pulse energies.

Acknowledgements

This research was financially supported by the Defence Threat Reduction Agency (through HDTRA1-12-1-0019 and HDTRA1-13-1-0019).